

# 1 Influence of biomass aerosol on precipitation over the Central 2 Amazon: An observational study

3

4 **W. A. Gonçalves<sup>1</sup>, L. A. T. Machado<sup>1</sup> and P-E, Kirstetter<sup>2</sup>**

5 [1]{ National Institute for Space Research-INPE/ Center for Weather Forecasting and Climate  
6 Studies–CPTEC, Cachoeira Paulista, SP, Brazil }

7 [2]{Advanced Radar Research Center/ University of Oklahoma and NOAA National Severe Storm  
8 Laboratory, Oklahoma, United States }

9 Correspondence to: W. A. Gonçalves (goncalves.weber@gmail.com)

10

## 11 **Abstract**

12 Understanding the influence of biomass burning aerosol on clouds and precipitation in the Amazon  
13 is key to reducing uncertainties in simulations of climate change scenarios with regard to  
14 deforestation fires. Here, we associate rainfall characteristics obtained from an S-Band radar in the  
15 Amazon with *in situ* measurements of biomass burning aerosol for the entire year of 2009. The  
16 most important results were obtained during the dry season (July-December). The results indicate  
17 that the influence of aerosol on precipitating systems is modulated by the atmospheric degree of  
18 instability. For less unstable atmospheres, the higher the aerosol concentration is, the lower the  
19 precipitation is over the region. In contrast, for more unstable cases, higher concentrations of black  
20 carbon are associated with greater precipitation, increased ice content, and larger rain cells; the  
21 finding suggests an association with long-lived systems. The results presented are statistically  
22 significant. However, due to limitations imposed by the available dataset, important features such as  
23 the contribution of each mechanism to the rainfall suppression need further investigation. Regional  
24 climate model simulations with aircraft and radar measurements would help clarify these questions.

25

## 26 **1 Introduction**

27 Every year, the Amazon forest faces a large amount of aerosol pollution from pasture and forest  
28 fires, and the generated pollution plumes can spread over large areas (Martin et al., 2010). The  
29 biomass burning aerosol (BBA) in the Amazon can alter atmospheric particulate material  
30 composition (Ryu et al., 2007) and influence cloud formation, precipitation, and the radiation

31 budget (Artaxo et al., 2002; Lin et al., 2006; Tao et al., 2012; Camponogara et al., 2014). According  
32 to Tegen et al. (1997), BBA predominates in the mean annual aerosol optical thickness in the  
33 Amazon. The dry season, which occurs between July and December, is the period that faces greater  
34 biomass burning emissions (Artaxo et al., 2002; Altaratz et al., 2010; Martin et al., 2010;  
35 Camponogara et al., 2014). However, from January to June (the wet period), BBA is also observed  
36 in the Amazon basin (Martin et al., 2010).

37 In recent years, the scientific community has made great efforts to understand the effect of aerosols  
38 on clouds and precipitation to reduce uncertainties in climate prediction (Tao et al., 2012). Two  
39 main effects are well documented: radiative or semi-direct, and microphysical or indirect effects.  
40 The first effect is related to BBA's high capacity for absorption in the visible portion of the  
41 electromagnetic spectrum (Hansen et al. 1997; Ramanathan et al. 2001; Wake, 2012). This  
42 absorption could warm the atmosphere (Koren et al., 2004; Randles and Ramaswamy, 2010; Koch  
43 and Del Genio, 2010; Jacobson, 2014) and produce atmospheric stabilization (Johnson et al. 2004;  
44 Koren et al. 2008). The semi-direct effect alters the atmospheric temperature in the boundary layer  
45 depending on the level at which the aerosol is presented (Randles and Ramaswamy, 2010). Johnson  
46 et al. (2004) commented that in cases of absorbing aerosol located above the boundary layer, the  
47 effect is the opposite, i.e., that the boundary layer suffers a radiative cooling. Boundary layer  
48 warming only occurs when the absorbing aerosols are constrained in the low atmosphere. The  
49 indirect or microphysical effect is linked to the possibility of BBA particles becoming cloud  
50 condensation nuclei (Roberts et al. 2001). As a result, it is expected that the quantity of cloud  
51 droplets would increase with the particle concentration (Rosenfeld, 1999; Ramanathan et al., 2001;  
52 Andreae et al., 2004; Qian et al., 2009).

53 One of the most important issues regarding the analysis of aerosol-cloud interactions is the  
54 determination of the predominant effect, radiative or microphysical. In warm rain suppression  
55 conditions, both effects seem to act together. However, the quantification of their respective  
56 contributions remains an important issue. Warm rain suppression evidence was firstly documented  
57 by Rosenfeld (1999), and similar results have subsequently been presented in the literature, e.g.,  
58 Koren et al., (2004) and Qian et al., (2009). The physical mechanism suggested for warm rain  
59 suppression is related to the fact that BBA has the potential to act as cloud condensation nuclei.  
60 Thus, in polluted environments, a large number of small cloud droplets could form (Rosenfeld,  
61 1999; Ramanathan et al., 2001; Andreae et al., 2004; Qian et al., 2009), which compromises the  
62 coalescence process (Borys et al., 2000; Hudson and Yum, 2001; McFarquhar and Heymsfield,  
63 2001; Yum and Hudson, 2002; Borys et al., 2003; Hudson and Myshra, 2007; Kaufman et al.,  
64 2005). These droplets do not reach the required size to precipitate and can rapidly evaporate due to

65 the semi-direct effect (Artaxo et al., 2006). However, as previously mentioned, the atmospheric  
66 level at which the BBA is located could lead to different results. Even a boundary layer cooling is  
67 likely to be observed. This could explain some of the controversy in the literature. Kaufman et al.  
68 (2005) and Brioude et al. (2009), for example, obtained results that differed from those  
69 demonstrated in other warm rain suppression publications. In these studies, the authors observed an  
70 increase in stratiform cloud formation in atmospheres with an elevated presence of aerosols.

71 In addition to the influence of BBA on warm rain, ice-phase cloud development is affected in  
72 polluted environments. In fact, laboratory measurements indicate a high capacity for ice nucleation  
73 by BBA (Petters et al., 2009). In recent years, some studies have suggested that ice-phase clouds are  
74 invigorated by the presence of aerosols from vegetation fires (Andreae et al., 2004; Lin et al., 2006;  
75 Rosenfeld et al., 2008; Altaratz et al., 2010; Koren et al., 2012; Storer and Heever, 2013). Rosenfeld  
76 et al. (2008) have proposed a conceptual model based on the effect of aerosols on deep convective  
77 cells, one that is mainly associated to the microphysical effect. According to the authors, due to the  
78 high concentration of aerosols in polluted environments, raindrop nucleation would be slower than  
79 in unpolluted areas. This process delays the initiation of precipitation, leading the droplets and  
80 aerosols to ascend into the atmosphere and reach the frozen layer. In addition, these droplets and  
81 aerosols could act as ice nuclei and release latent heat, which could increase the updrafts and  
82 invigorate the cloud dynamics (Lin et al. 2006; Rosenfeld et al. 2008). However, even with this  
83 evidence, the cloud invigoration process by aerosols still needs to be better understood (Altaratz et  
84 al., 2014).

85 Although well documented, particularly in recent studies, the BBA effect on clouds and  
86 precipitation is still a source of debate in the scientific community. One of the most important  
87 outstanding issues is related to filtering the aerosol-precipitation relationship from other dominant  
88 atmospheric processes. To reach this goal, this study presents a new methodology based on the  
89 atmospheric degree of instability. The use of ground-based measurements has the potential to  
90 contribute to the present scientific knowledge on the influence of BBA on precipitating cells in the  
91 Amazon region. Parameters of rain, ice content, size and duration of precipitating systems retrieved  
92 from an S-band radar were evaluated as functions of black carbon (BC) concentration over the  
93 largest Amazon city (Manaus, Amazonas state, Brazil).

94

## 95 **2 Data analysis**

96 All analyses performed in this study were performed using a combination of four datasets:

97 1) Terrain elevation data at a  $90 \times 90$  m<sup>2</sup> resolution from the Shuttle Radar Topography Mission  
98 (SRTM);

99 2) Weather radar data from the Manaus S-Band Doppler Radar ( $1 \times 1 \text{ km}^2$  horizontal resolution in a  
100 range of 100 km, updated every 11 min);

101 3) BC concentration data from the European Integrated Project on Aerosol Cloud Climate and Air  
102 Quality Interactions (EUCAARI) experiment, with a sampling time of 1 min and averaging every  
103 30 min. The EUCAARI experiment used the Multi-Angle Absorption Photometer (MAAP)  
104 instrument (Slowik et al., 2007) and collected data 50 km away from Manaus city. The BC  
105 concentrations were used in the study as aerosol tracer data;

106 4) Atmospheric soundings from the Manaus station. The atmospheric soundings were used to  
107 calculate the Convective Available Potential Energy (CAPE), an important atmospheric index used  
108 as an intense convective activity predictor (Wallace and Hobs, 2006). As Manaus radiosondes were  
109 released by an operational station, only soundings at 00:00 and 12:00 UTC, 08:00 and 20:00 local  
110 time, were available. The most appropriate time for a sounding in this study is approximately noon,  
111 when convection starts to develop in the area. However, the CAPE dataset was evaluated and  
112 shown to have substantially useful information and ability to capture daily instability features even  
113 though the recordings were not made at the most appropriate times. The 08:00 local time soundings  
114 also presented a considerable population of high CAPE values (greater than  $2600 \text{ J/Kg}$ ). In addition,  
115 more than 70 % of the days that had CAPE values higher than  $2600 \text{ J/Kg}$  at 00:00 UTC presented  
116 high CAPE values the next morning (as measured at 12:00 UTC).

117 Notably, BC is a byproduct of the partial combustion of fossil fuels or a remnant from wildfires  
118 (Ahmed et al., 2014), and it represents only approximately 5 % of the total carbon concentration  
119 resulting from biomass burning (Formenti et al., 2001; Graham et al., 2003; Cozic et al., 2008).  
120 However, BBA dominates the aerosol concentration in the Amazon basin, allowing for the use of  
121 BC as an aerosol tracer. BC concentration is well correlated with aerosol concentration in Amazon.  
122 Several studies in Amazonia have demonstrated this relationship. Bevan et al. (2009) used a 13-year  
123 time series of Along Track Scanning Radiometer (ATSR)-derived aerosol optical depth (AOD)  
124 measurements to examine the role of aerosol in the interaction with biomass burning over the  
125 Amazon. AOD has a significant positive correlation with the total number of satellite-observed  
126 fires. Additionally, numerous studies have used aerosol particles greater than 80 nm as a proxy for  
127 cloud condensation nuclei (CCN). Andrea et al. (2008) and Liu and Li (2014) commented on the  
128 positive relationship between aerosol concentrations and CCN.

129 BC has received attention by the scientific community due to its potential for ice nucleation, which  
130 can affect the microphysical properties of clouds (Cattani et al., 2006; Cozic et al., 2008). The  
131 supersaturation required for ice formation decreases with the presence of BC (DeMott et al., 1999).  
132 Cozic et al. (2008) found that a portion of the cloud droplet nuclei present in mixed-phase clouds

133 comprises BC. Therefore, due to its potential for ice nucleation, the presence of BC would favor the  
134 invigoration of pre-existing ice-phase clouds, including deep convection. As discussed previously,  
135 BC also has the capacity to absorb radiation in the visible portion of the electromagnetic spectrum  
136 (Ramanathan et al., 2001; Storelvmo, 2012; Tiwari et al., 2013; Ahmed et al., 2014). This  
137 characteristic could warm the layer where BC is present (Myhre, 2009; Mahowald, 2011; Jones et  
138 al., 2011; Wake, 2012; Wang, 2013), which could stabilize the atmosphere and reduce the formation  
139 of cumulus clouds. In turn, this characteristic of BC could also affect cloud properties and  
140 precipitation indirectly as discussed above.

141 The S-band radar data were processed following the TRADHy strategy (Delrieu et al. 2009), briefly  
142 described hereafter. A preliminary quality control of the radar data was performed, and the radar  
143 calibration was checked throughout the year 2009. The area actually sampled by the radar was  
144 determined for each elevation angle along with a characterization of partial or complete beam  
145 blockage and ground clutter. Rain types and the corresponding vertical profiles of reflectivity  
146 (VPRs) were dynamically identified. Regarding VPR identification, the initial method used in  
147 TRADHy performs a numerical identification of VPRs from the comparison of the radar data at  
148 different distances and altitudes to account for sampling effects (Kirstetter et al., 2010). In the  
149 present study, the physical approach described by Kirstetter et al. (2013) was used to identify with  
150 enhanced robustness a representative VPR over the radar domain for a given precipitation type.  
151 Corrections for both clutter and beam blockage were performed along with a projection of  
152 measured reflectivities onto the ground level using rain-typed VPRs. At a given pixel, reflectivities  
153 from all available elevation angles were used for the projection. The projected radar reflectivity of a  
154 constant altitude plan at the same elevation as the radar was called the Constant Altitude Plan  
155 Position Indicator-Ground (CAPPI-Ground). The Vertical Ice Content (VIC) for each pixel of the  
156 radar images was also calculated. The method described in Kirstetter et al. (2013) is based on a  
157 modeling of the physical properties of the hydrometeors (size distribution, shape, phase,  
158 electromagnetic properties, etc.) contributing to the VPR features. In particular the model for the ice  
159 phase above the freezing level allows for the computation of the VIC. The identified VPR is then  
160 associated to a model for the ice phase, which is used to compute the VIC at each pixel alongside  
161 the projection of reflectivity at the surface.

162 To determine the general behavior of precipitation in the study area, as well as its relationship with  
163 particulate material, three indices were used as follows:

$$164 \quad \text{RF} = N_{20 \text{ dBZ}} / N_{\text{TOTAL}} \times 100 \quad (1)$$

$$165 \quad \text{IRF} = N_{45 \text{ dBZ}} / N_{\text{TOTAL}} \times 100 \quad (2)$$

166  $IF = N_{1\text{ mm}} / N_{\text{TOTAL}} \times 100$  (3)

167 where

168 – RF is the Rain Fraction;

169 – IRF is the Intense Rain Fraction;

170 – IF is the Ice Fraction;

171 –  $N_{20\text{ dBZ}}$  is the number of CAPPI-Ground pixels with a reflectivity equal or higher than 20 dBZ;

172 –  $N_{45\text{ dBZ}}$  is the number of CAPPI-Ground pixels with a reflectivity equal or higher than 45 dBZ;

173 –  $N_{1\text{ mm}}$  is the number of VIC pixels equal or higher than 1 mm;

174 –  $N_{\text{TOTAL}}$  is the sum of pixels in the area.

175 The three indices described above indicate the spatial distribution of the rain properties in the study  
176 domain. The higher their value, the greater the part of the study area covered by the physical  
177 property analyzed. The RF and IRF indices express how the rain and the intense rain are distributed  
178 in the domain according to the respective thresholds of 20 and 45 dBZ, which approximately  
179 correspond to rain rates of  $1\text{ mmh}^{-1}$  and  $30\text{ mmh}^{-1}$ , respectively, according to Marshall and Palmer  
180 (1948). IF indicates the percentage of the area covered by ice clouds. As previously described, the  
181 value of 1 mm was chosen from the VPR method to determine IF. Note that the procedure was  
182 tested with higher VIC values. However, the number of samples was observed to decrease  
183 drastically, leading us to choose the value of 1 mm. Petersen et al. (2005) showed that this value  
184 corresponds to the beginning of a relationship between vertical ice content and lightning flash  
185 density.

186 The algorithm known as Forecast and Tracking the Evolution of Cloud Clusters (FORTRACC),  
187 described in detail by Vila et al. (2008), is capable of tracking the evolution of cloud systems.  
188 Originally, FORTRACC was applied on infrared images from geostationary meteorological  
189 satellites. The FORTRACC version used in this study is adapted to meteorological radars.  
190 FORTRACC was used to describe the size and duration of the rain cells. CAPPI-Ground images  
191 were used to track rain cells around the city of Manaus; cells were defined using the 20 dBZ  
192 threshold.

193 As presented previously, the datasets do not share the same temporal sampling frequency. A  
194 methodology was applied to collocate them in time. All variables derived from the radar samples  
195 (RF, IRF, IF, and size and duration of the rain cells) were collected from the atmospheric soundings  
196 within  $\pm$  two hours of each other. This consideration was made because only two atmospheric  
197 soundings were available during each day. As a result, the atmospheric stability, inferred by CAPE,

198 was considered constant within  $\pm$  two hours of the sounding launch time. The BC concentrations  
199 with the closest measurement times to the radar data were used. This temporal matching of the  
200 variables allowed us to understand the aerosol effect on precipitation in the Amazon basin.

201

### 202 **3 The seasonal evolution of black carbon concentration and convective processes**

203 The Manaus precipitation characteristics were obtained from the RF and IRF data. The RF and IRF  
204 values were normalized by their annual means and standard deviations to compare both annual  
205 cycles. The result (Fig. 1a) was useful in determining two distinct periods with which to perform  
206 the analysis. Months during which the normalized RF value was greater or smaller than zero were  
207 considered to comprise the rainy or dry seasons, respectively. The period between January and June  
208 was identified as the rainy season, and the period between July and December as the dry season.  
209 From previous studies, it is known that a strong increase in the level of precipitation occurs in the  
210 months of November and December. However, in our analysis, only a slight increase in the  
211 normalized RF was observed (Fig. 1a). This behavior could be attributed to an observed El Niño  
212 configuration, which potentially decreases the precipitation in the Amazon. Another important  
213 aspect is that the normalized IRF value is higher within the dry period (Fig. 1a). The frequency of  
214 intense precipitation increases mainly toward the end of the dry season. This increase is related to a  
215 reduction in the inversion layer and an increase in CAPE and moisture due to the monsoon  
216 circulation (Machado et al., 2004). This result indicates that in the dry period, when large-scale  
217 precipitation decreases in the study area, most of the precipitation is related to intense convection,  
218 which mainly occurs over elevated areas.

219 Even with small variations of terrain elevations, with the highest point at approximately 160 m, a  
220 notable precipitation feature within the study domain is found to be related to the topography (Fig.  
221 2). For the rainy period (Fig. 2a), all of the elevations had a reflectivity peak greater than 20 dBZ  
222 (approximately  $1 \text{ mm h}^{-1}$ ). In other words, precipitation occurs in a nearly spatially homogeneous  
223 manner during the rainy season despite a high peak of reflectivity observed over elevated regions.  
224 During the dry season (Fig. 2b), reflectivity peaks greater than 20 dBZ were only observed over  
225 elevated areas. This suggests that in the absence of a large scale circulation that could support the  
226 precipitation, the upslope triggering plays an important role in the formation of rain cells.  
227 Importantly, the two last categories of elevations presented in Fig. 2 are more than 60 km from the  
228 radar. At this distance, the lower radar elevation band is approximately 1 km high, which eliminates  
229 the possibility of effects from ground clutter. An important test was performed to ensure that the  
230 influence of topography on the rain systems would not lead to misinterpretations of the aerosol–  
231 precipitation relationship. Details of this test are presented in Section 4.

232 In addition to precipitation characteristics, the annual cycle of BC concentration (Fig. 1b) was  
233 considered for separating the analyses into rainy/dry periods. During the rainy season, the BC  
234 concentration was below  $700 \text{ ng m}^{-3}$  for almost the entire period. This low concentration could be  
235 explained by wet deposition or the absence of large sources of biomass burning (Martin et al.,  
236 2010). On the other hand, for the other six months, the BC concentration increased, mainly due to a  
237 high number of deforestation fires in the region (Artaxo et al., 2006) and a decrease in the observed  
238 precipitation. This characteristic favors the outbreak of fires in the forest, allowing them to spread  
239 over the region.

## 240

## 241 **4 The effect of instability on the rainfall–aerosol relationship**

### 242 **4.1 Observational Evidence**

243 The first analysis focused on the overall relationship between BC concentrations and the rain  
244 characteristics (Fig. 3). At this stage, no consideration was made regarding the filtering of a possible  
245 BBA effect on precipitation from another atmospheric feature. For the rainy period (Fig. 3b), a  
246 decrease in RF was observed as BC concentration increased. In contrast, during the dry period (Fig.  
247 3c), a decrease in RF was observed up to approximately  $1000 \text{ ng m}^{-3}$  of BC. Beyond this value, the  
248 RF slightly increased. Although it was not statistically significant, this characteristic led us to  
249 attempt a filtering out of the possible aerosol influence on precipitation from an atmospheric feature  
250 that could modulate this effect. At this stage, CAPE was chosen as the atmospheric component.  
251 Therefore, the precipitation/BC comparisons were performed for less unstable ( $\text{CAPE} < 1400 \text{ J kg}^{-1}$   
252 <sup>1</sup>, i.e., less convective activity) and more unstable ( $\text{CAPE} > 2600 \text{ J kg}^{-1}$ , i.e., more convective  
253 activity) atmospheres. These values are similar to those presented by Wallace and Hobbs (2006),  
254 and found to be appropriate for dividing the convective activity according to the CAPE value.

255 A test was applied prior to the study to determine whether the scavenging process was significant in  
256 the study area. The main objective of this study was to identify the influence of BBA on  
257 precipitation. However, precipitation can also modify BBA concentrations in the atmosphere, due to  
258 the wet scavenging process. As mentioned previously, the BC measurements were made *in situ*,  
259 approximately 50 km from the city of Manaus, in the state of Amazonas. Thus, the concept of this  
260 test was based on eliminating from our statistics all samples for which precipitation was observed  
261 over the EUCAARI site. This filtering excluded the samples in which precipitation could have  
262 cleaned the atmosphere, throughout the scavenging process. After this, comparisons between the RF  
263 and BC concentrations were performed. No significant differences were observed when comparing  
264 the results utilizing this criterion with those in which no consideration was given to a potential  
265 aerosol wet scavenging effect. This characteristic indicates that the local scavenging effect seems to



266 be of a second order on the BC-rain interaction. However, this test does not take into account the  
267 reduction of BC sources outside the measurement site due to rainfall. Therefore, it is not possible to  
268 separate the scavenging effect from other physical effects associating reduction of rainfall with the  
269 increase in BC concentration, even if the scavenging effect seems to be of a second order, locally. In  
270 addition, Gryspeerdt et al. (2015) commented that the time difference between the measurements of  
271 rain properties and aerosol could lead to misinterpretations in the aerosol-rainfall relationship, as  
272 the timescale of wet scavenging is narrow. In this study, the temporal sampling frequency difference  
273 between the EUCAARI and radar measurements is five minutes in the worst case scenario. This  
274 sampling time difference, though minor, could have allowed the scavenging effect to remain even  
275 with the use of the described test.

276

277 As described in Section 3, terrain elevation plays an important role in triggering precipitation in the  
278 region, mainly during the dry season (Fig. 2b). In the statistical analyses performed herein, no  
279 consideration was made for the topography in the analysis of the BC-precipitation relationship.  
280 However, to make sure that no considerations were necessary, a relevant test was performed to  
281 avoid misinterpretations of the conclusions regarding the comparisons between the rainfall  
282 characteristics and their association with BC concentrations. This test was conducted to verify  
283 whether the BC-precipitation relationship was different for each topography category presented in  
284 Fig. 2. For each category, we compared the RF values for different BC concentrations in less and  
285 more unstable atmospheres. The results for each terrain elevation category were statistically similar  
286 to the statistical analyses described below. Therefore, though important for triggering precipitation,  
287 the elevation did not influence the results related to BC-precipitation comparisons, which allowed  
288 us to use all grid points in our study independently of their elevation.

289 The two important tests previously described help to reinforce the evidence of the influence of BBA  
290 on the rainfall characteristics presented hereafter. During the wet period, no differences were  
291 observed for the less and more unstable cases. The behavior was identical to that obtained when no  
292 atmospheric considerations were performed (Fig. 3b). A similar pattern was observed for the less  
293 unstable cases during the dry season (Fig. 4a). In support of this result, the RF distributions (Fig.  
294 4c) presented a more elongated tail for the small BC concentrations. This decrease could be  
295 associated with the suppression of warm or stratiform precipitation because it is unlikely that a  
296 strong convection could form in stable cases. The exact opposite behavior was found for the more  
297 unstable atmospheres within the dry period (Fig. 4b). The RF increased in cases where higher  
298 concentrations of BC were observed. The precipitation appeared to spread over the region when the  
299 atmosphere was favorable to the development of convection associated with BBA. The distribution

300 of RF for three categories of BC (Fig. 4d) shows that the greater the particulate material  
301 concentration, the more elongated the tail of the RF distributions. As commented in Section 2, RF is  
302 an indication of the distribution of rain in the study domain. Therefore, an increase in values for this  
303 variable for polluted atmospheres does not necessarily mean that more intense convection is  
304 occurring. However, this behavior was observed when the atmosphere presented conditions for  
305 intense convection. Consequently, this result could be an indication that convection is invigorated  
306 by higher BBA concentrations (Lin et al., 2006; Graf, 2004; Rosenfeld et al., 2008; Altaratz et al.,  
307 2010; Koren et al., 2012) when the atmosphere is highly unstable (i.e., presenting high CAPE  
308 values).

309 An analysis evaluating the presence of ice in the precipitating cells within polluted atmospheres has  
310 the potential to give support to the previously described evidence. Therefore, to understand whether  
311 the amount of cloud ice is influenced by the presence of high BBA concentrations, the IF index was  
312 calculated based on Eq. 3. This procedure was important to account for the fact that ice formation  
313 could be influenced by BC (Demott et al., 1999; Cozic et al., 2008; Kireeva et al., 2009). In addition  
314 to the convective case hypothesis, we verified whether the precipitation suppression observed for  
315 the less unstable case could link to the presence of stratiform clouds. The mean IF values decreases  
316 substantially in proportion to the increase in BC concentration for less unstable atmospheres (Fig.  
317 5a). This result could be an indication that stratiform clouds are negatively influenced by BBA. In  
318 more unstable cases, the result indicates that the convection invigoration hypothesis (Rosenfeld et  
319 al., 2008) based on the presence of aerosols is likely to be true (Fig. 5b), in agreement with the RF-  
320 BC relationship previously indicated.

321 The RF-IF/BC analyses were useful for understanding the increase/decrease in precipitation or ice  
322 fraction over the entire radar coverage area. However, they do not give information on the space  
323 and time scale organization of the rainfall. FORTRACC was employed to evaluate whether BBA  
324 changes the lifetime duration of the rain cells. First, rain cells resulting from splitting or merging  
325 were eliminated from the data for the duration analysis. In fact, splitting or merging modify the  
326 physical characteristics of the precipitating systems, influence their duration, and compromise the  
327 evaluation of the BBA effect on them. In addition, rain cells that do not have their entire lifecycle  
328 inside the radar domain were not considered, as it was not possible to determine the lifetime of a  
329 rain cell that did not initiate and dissipate inside the radar domain. These filters drastically decrease  
330 the sample of rain cells analyzed. The results showed no significant change in the lifetime duration  
331 as a function of BBA. Unfortunately, the lifecycle rain cell population was not statistically  
332 significant after all these considerations. However, the study of the rain cell size distributions is not  
333 subject to any of these limitations, and all rain cells, regardless of whether they had their entire

334 lifecycle inside the domain region, can be taken into account. For the rainy season, no significant  
335 effect was observed on the rain cell size relationship with the BC concentration. The same pattern  
336 was observed for the dry season, except for rain cells larger than 100 km<sup>2</sup> in more unstable  
337 atmospheres. For systems smaller than 100 km<sup>2</sup>, even in high instability cases, the increase in BC  
338 concentration does not exhibit any significant relationship with rain cell size. However, for larger  
339 rain cells (Fig. 6a), in unstable atmospheres during the dry season, the rain cell size increases as a  
340 function of the BC concentration. Although a large variability can be noted in Fig. 6, the tail of the  
341 rain cell size distribution shows a larger size for higher BC concentrations (Fig. 6b). Moreover, the  
342 curves are significantly different as determined using a t-test with a 95% confidence level. The  
343 presence of particulate material appears to reinforce the convection that is well established by the  
344 increased level of atmospheric instability. The mean system area increases from 300 to over 900  
345 km<sup>2</sup> as BC concentration varies from 300 to 1660 ng m<sup>-3</sup>.

346

#### 347 **4.2 Discussion of the possible physical mechanisms**

348 In our analyses, we observed that polluted atmospheres are generally associated with decreased  
349 precipitation. This behavior was also evident for the dry season in less unstable atmospheres.  
350 However, during the dry season in more unstable atmospheres, RF and IF increase as BC  
351 concentration increases. In this section we discuss some physical mechanisms potentially related to  
352 these observations. Although it was not possible to evaluate the cloud droplet size distribution with  
353 the dataset used in this study, a mechanism responsible for the observed behavior can still be  
354 suggested. The decreases in RF and IF with increasing BC could be related to enhanced formation  
355 of cloud droplets with reduced size (Rosenfeld, 1999; Ramanathan et al., 2001), compromising the  
356 coalescence process (Kaufman et al., 2005). In the absence of strong buoyancy, the small droplets  
357 do not ascend to high atmospheric levels, and evaporate easily or do not develop to a rainfall drop  
358 size, in a mechanism similar to warm precipitation suppression. The wet scavenging process, an  
359 important component responsible for the removal of aerosol in the atmosphere, could also  
360 contribute to the results observed, mainly for lower BC concentrations, at which the RF and IF  
361 reach their higher values. Moreover, it is not possible to define which effect (semi-direct or indirect)  
362 dominates or what the feedback between them is. As the RF and IF decrease for elevated BC  
363 concentrations, the dominant effect could be explained by the wet deposition theory and/or the rain  
364 suppression theory. In addition, the radiative effect acts to increase the population of stable  
365 atmosphere cases and results in less rainfall for the situation of high aerosol loading.

366 During the dry season, in a more unstable condition, our results indicate an invigoration of the  
367 precipitation with increasing BC concentration. Considering that high CAPE values are associated

368 with stronger updrafts, the aerosol effect on the rainfall and on the severity of the convective  
369 processes could depend on the intensity of the vertical motions. In addition, it is important to note  
370 that during the dry season, only elevated regions trigger convection, which could support the  
371 intensification of the updrafts in more unstable atmospheres. The radiative effect, which also acts to  
372 stabilize the atmosphere, is probably of a second order. Even with high levels of BBA, the  
373 atmosphere is highly unstable, and thermodynamics on this time scale seem to dominate over the  
374 radiative process. Additionally, an increase in the droplet evaporation process, which could be  
375 generated by the radiative effect, does not seem to be the predominant mechanism. Probably due to  
376 the high instability (high updraft), the large number of small droplets inside clouds (formed by the  
377 microphysical effect) ascend very fast, thereby reducing the extent of evaporation. Rosenfeld et al.  
378 (2008) commented that an unstable atmosphere could carry the small droplets to higher atmospheric  
379 levels, invigorating convection and increasing the amount of ice. Moreover, BC particles could be  
380 carried within the updrafts and act as ice nuclei. During the dry season, most of the precipitation is  
381 associated with elevated regions, and in the more unstable cases, it appears that BBA helps to  
382 increase ice nuclei formation and precipitation. Although impossible to quantify, the wet scavenging  
383 process also seems to be of second order. It would act in the opposite direction through the fact that  
384 RF and IF are higher for polluted atmospheres (Figs. 4b and 5b). Notably, however, it is possible  
385 that for small IF and RF values, the effect of the wet scavenging process is still present in the  
386 statistical analyses. In these cases, the applied wet scavenging test may not have been able to  
387 identify this process. The last result presented in the previous section was related to the  
388 consequence of the BBA loading on the size of the precipitating systems. Agreeing with the RF/IF  
389 analyses, polluted atmospheres seem to influence the development of larger precipitating systems  
390 for the more unstable cases in the dry season. However, as commented before, this effect was only  
391 observed for systems larger than 100 km<sup>2</sup>. This result is probably due to the entrainment effect,  
392 which depends inversely on cloud radii in the updrafts (Simpson and Wiggert, 1969). Larger rain  
393 cells have smaller entrainment, favoring higher levels of neutral buoyancy. Storelvmo (2012) also  
394 commented that the entrainment rate plays an important role on the aerosol effect on deep  
395 convective clouds. In addition, it is important to note that Koren et al. (2012) observed that rain  
396 cells occurring under polluted conditions had their coverage area increased by approximately 20 %,  
397 which also lends support to the results presented in this research. The main results presented in this  
398 study and the mechanisms proposed are summarized in Table 1.

399

## 400 **5 Conclusions and discussions**

401 This study evaluates the relationship between precipitation and BC concentration using data from

402 one year of ground observations. The results presented are innovative and independent; most prior  
403 studies have relied on satellite remote sensing. The methodology using observational data presented  
404 herein may contribute to the knowledge of the BBA effect on precipitating systems in the Amazon  
405 basin. One of the greatest difficulties regarding this issue has been filtering the aerosol effect from  
406 other important atmospheric features. Large-scale circulation or thermodynamic effects represent a  
407 major component underlying the strengthening of convection. An analysis of the contribution of  
408 each effect could not be performed observationally, but through theoretical simulations that are not  
409 completely parameterized. In this study, CAPE values were used as the atmospheric filtering  
410 component, which allowed us to divide analyses according to the degree of atmospheric stability.  
411 Important features, such as wet scavenging, synoptic scale influence, and droplet size distribution  
412 characteristics, need further study and improvement to extend this result. As BBA is predominant in  
413 the Amazon basin, BC was used as an aerosol tracer. Nevertheless, other types of aerosol are also  
414 present in the region and should receive more attention in new field campaigns. The El Niño  
415 configuration, as was observed during the dry season, is associated with reduced levels of  
416 precipitation and a decrease in the occurrence of rain cells. Even if this situation had decreased the  
417 rain cell population used to study the lifetime duration, a significant number of samples were  
418 analyzed for the evaluation of the aerosol-rainfall interaction, and this did not compromise the main  
419 results of this study that are associated with the convective scale.

420 Despite the limitations of the database and the large set of independent variables, the results  
421 presented in this study were statistically significant and physically relevant. BBA releases into the  
422 atmosphere generally appear to contribute to a decrease in precipitation. It has been difficult to  
423 define the main factor responsible for this behavior because there are several effects, such as wet  
424 scavenging or atmosphere inhibitions, which cannot be excluded from the results and could also  
425 contribute to precipitation reduction. Nevertheless, we postulate a probable physical mechanism  
426 that could explain the observed results as follows. The decrease of RF and IF could be associated to  
427 the warm rain suppression mechanism linked to the radiative effect, or to an association of the  
428 radiative and microphysical effects together. The most important result obtained in this research was  
429 the difference in the rain features analyzed during the dry season for less and more unstable  
430 atmospheres. The convective invigoration of polluted atmospheres was only observed in more  
431 unstable atmospheres. This appears to be a considerably significant result, based on the fact that the  
432 wet scavenging process acts in the opposite direction, reducing precipitation. The wet scavenging  
433 appears to be of a second order in the precipitation-aerosol relationship for elevated concentrations  
434 of BC. However, it was only possible to obtain a qualitative result because it was not possible to  
435 isolate this process for the precipitation inhibition cases and quantify the exact effect on the rain and  
436 ice fractions. Based on the results, we could again postulate a probable physical mechanism which

437 could explain the observed behavior. We observed that during the dry season, most convection  
438 occurs in elevated areas. Thus, in more unstable cases, stronger updrafts inside the rain cells  
439 initiated over those elevated regions probably carry a greater quantity of droplets formed in a  
440 polluted environment to high tropospheric levels, producing in the clouds changes related to their  
441 microphysical properties, dynamics and thermodynamics. We were unable to measure the quantity  
442 of droplets formed due to the microphysical effect, and the vertical velocity within the precipitating  
443 systems was not available in the database used. However, the vertical velocity can be directly linked  
444 to CAPE values because the greater the atmospheric instability is, the stronger the updrafts are. This  
445 study does not define any specific BC concentration that could activate the cloud process, possibly  
446 increasing convective strengthening. Nevertheless, it has been shown that this process only occurs  
447 significantly when the BC concentration is higher than  $1200 \text{ ng m}^{-3}$ .

448 The indication of the influence of BBA on the size of the rain cells followed the same behavior  
449 observed for RF and IF. We again suggest that the effect is modulated by the atmospheric degree of  
450 instability. An important size threshold was found, and the relationship between BC concentration  
451 and rain cells area seems to depend on it. The influence of BBA on convective strengthening was  
452 observed for large rain cells. This effect is probably related to the reduced entrainment of dry air  
453 parcels into the convection, favoring a higher level of neutral buoyancy. The area increase was only  
454 observed for systems larger than  $100 \text{ km}^2$  for the more unstable cases in the dry period. Although  
455 the analysis of the influence of BBA on the longevity of the rain cells has been inconclusive, some  
456 evidence of this relationship should be mentioned. It is well known that the size of rain cells is  
457 positively correlated to their longevity. Thus, the results presented in this study could be an  
458 indication that high concentrations of BC could lead to longer lifetime rain cells, depending on the  
459 atmospheric degree of instability.

## 460 **Acknowledgements**

461 This study was funded by the following grants: CNPq-141952/2010-5 and FAPESP-CHUVA  
462 Project 2009/15235-8. We thank Paulo Artaxo for the discussions and for providing the EUCAARI  
463 database and the Amazon Protection National System (SIPAM) for the S-Band radar dataset.

464

465 **References**

- 466 Ahmed, T., Dutkiewicz, V. A., Khan, A. J., Husain, L.: Long term trends in Black Carbon  
467 Concentrations in the Northeastern United States, *Atmospheric Research*, 137, 49-57,  
468 2014.
- 469 Altaratz, O., Koren, I., Yair, Y., Price, C.: Lightning response to smoke from Amazonian  
470 fires, *Geophys. Res. Lett.*, 37, 1-6, L07801, doi:10.1029/2010GL042679, 2010.
- 471 Altaratz, O., Koren, I., Remer, L. A., Hirsch, E.: Review: Cloud invigoration by aerosols-  
472 Coupling between microphysics and dynamics, *Atmospheric Research*, 140–141, 38–60,  
473 2014.
- 474 Andrea, S. D., Hakkinen S. S. K., Westervelt, D. M., Kuang, C., Levin, E. J. T., Kanawade,  
475 V. P., Leitch, W. R., Spracklen, D. V., Riipinen, I, Pierce, J. R.: Understanding global  
476 secondary organic aerosol amount and size-resolved condensational behavior. *Atmos.*  
477 *Chem. Phys.*, 13, 11519–11534, 2013. doi:10.5194/acp-13-11519-2013.
- 478 Andreae, M. O., Rosenfeld, D., Artaxo, P., Costa, A. A., Frank, G. P., Longo, K. M., Silva-  
479 Dias, M. A. F.: Smoking rain cloud over the Amazon, *Science*, 303, 1337-1342, 2004.
- 480 Artaxo, P., Martins, J. V., Yamasoe, M. A., Procópio, A. S., Pauliquevis, T. M., Andreae, M.  
481 O., Gunyon, P., Gatti, L. V., Leal, A. M. C.; Physical and chemical properties of aerosols in  
482 the wet and dry seasons in Rondônia Amazônia, *J. Geophys. Res.*, 107,1-14, D20, doi:  
483 10.1029/2001JD000666, 2002.
- 484 Artaxo, P., Oliveira, P. H., Lara, L. L., Pauliquevis, T. M., Rizzo, L. R., Junior, C. P., Paixão,  
485 M. A.: Efeitos climáticos de partículas de aerossóis biogênicos emitidos em queimadas na  
486 Amazônia, *Revista Brasileira de Meteorologia*, 21, 168-189, 2006.
- 487 Bevan, S. L., P. R. J. North, W. M. F. Grey, S. O. Los, and S. E. Plummer.: Impact of  
488 atmospheric aerosol from biomass burning on Amazon dry-season drought, *J. Geophys.*  
489 *Res.*, 114, D09204, doi:10.1029/2008JD011112, 2009.
- 490 Borys, R. D., Lowenthal, D. H., Cohn, S. A., Brown, W. O. J.: Mountaintop and radar  
491 measurements of anthropogenic aerosol effects on snow growth and snowfall rate,  
492 *Geophys. Res. Lett.*, 30(10), 1538, doi:10.1029/2002GL016855, 2003.
- 493 Borys, R. D., Lowenthal, D. H., Mitchell, D. L.: The relationships among cloud  
494 microphysics, chemistry and precipitation rate in cold mountain clouds, *Atmos. Environ.*,  
495 34, 2593–2602, 2000.
- 496 Camponogara, G., Silva Dias, M. A. F., and Carrió, G. G.: Relationship between Amazon

497 biomass burning aerosols and rainfall over the La Plata Basin, *Atmos. Chem. Phys.*, 14,  
498 4397–4407, doi:10.5194/acp-14-4397-2014, 2014.

499 Cattani, E., Costa, M. J., Torricella, F., Levizzani, V., Silva, A. M.: Influence of aerosol  
500 particles from biomass burning on cloud microphysical properties and radiative forcing,  
501 *Atmospheric Research*, 82, 310–327, 2006.

502 Cozic, J., Mertes, S., Verheggen, B., Cziczo, D. J., Gallavardin, S. J., Walter, S.,  
503 Baltensperger, U., Weingartner, E.: Black carbon enrichment in atmospheric ice particle  
504 residuals observed in lower tropospheric mixed phase clouds, *Journal of Geophysical*  
505 *Research*, 113, 1-11, 2008.

506 Delrieu, G., Boudevillain, B., Nicol, J., Chapon, B., Kirstetter, P. E., Andrieu, H., and Faure,  
507 D.: Bollène 2002 experiment: radar quantitative precipitation estimation in the Cévennes-  
508 Vivarais region, France, *J. Appl. Meteorol.Clim.*, 48, 1428-1447, 2009.

509 DeMott, P. J., Chen, Y., Kreidenweis, S. M., Rogers, D. C., Sherman, D. E.: Ice formation  
510 by black carbon particles, *Geophys. Res. Lett.*, 26, 2429–2432, 1999.

511 Formenti, P., Andreae, M. O., Lange, L., Roberts, G., Cafmeyer, J., Rajta, I., Maenhaut,  
512 W., Holben, B. N., Artaxo, P., Lelieveld, J.: Saharan dust in Brazil and Suriname during the  
513 Large-Scale Biosphere-Atmosphere Experiment in Amazonia (LBA)–Cooperative LBA  
514 Regional Experiment (CLAIRE) in March 1998, *J. Geophys. Res.*, 106, 919-934, 2001.

515 Graf, H. F.: The complex interaction of aerosols and clouds, *Science*, 303, 1309-1311,  
516 2004.

517 Graham, B., Guyon, P., Taylor, P. E., Artaxo, P., Maenhaut, W., Glovsky, M. M., Flagan, R.  
518 C., and Andreae, M. O.: Organic compounds present in the natural Amazonian aerosol:  
519 characterization by gas chromatography-mass spectrometry, *J. Geophys. Res.*, 108, 1-13,  
520 D24, doi: 10.1029/2003JD003990, 2003.

521 Gruspeerd, E., Stier, P., White, B. A., Kipling, Z.: Wet scavenging limits the detection of  
522 aerosol-cloud-precipitation interactions. *Atmos. Chem. Phys. Discuss.*, 15, 6851–6886,  
523 2015. doi:10.5194/acpd-15-6851-2015

524 Hansen, J., Sato, M., and Ruedy, R.: Radiative forcing and climate response, *Journal of*  
525 *Geophysical Research*, 102(D6), 6831– 6864, 1997.

526 Hudson, J. G., and Mishra, S.: Relationships between CCN and cloud microphysics  
527 variations in clean maritime air, *Geophys. Res. Lett.*, 34, L16804,  
528 doi:10.1029/2007GL030044., 2007.



529 Hudson, J. G., and Yum S. S.: Maritime-continental drizzle contrasts in small cumuli, J.  
530 Atmos. Sci., 58, 915–926, 2001.

531 Jacobson, M., Z.: Effects of biomass burning on climate, accounting for heat and moisture  
532 fluxes, black and brown carbon, and cloud absorption effects, Journal of Geophysical  
533 Research, 2014.

534 Johnson, B. T., Shine, K. P., and Forster, P. M.: The semi-direct aerosol effect: Impact of  
535 absorbing aerosols on marine stratocumulus, Q. J. Roy. Meteorol.Soc., 130(599), 1407–  
536 1422, 2004.

537 Jones, G. S., Christidis, N., Stott, P. A.: Detecting the influence of fossil fuel and bio-fuel  
538 black carbon aerosols on near surface temperature changes, Atmospheric and Chemistry  
539 Physics, 11, 799-816, 2011.

540 Kaufman, Y. J., Koren, J. A., Remer, L. A., Rosenfeld, D., Rudich, Y.: The effect of smoke,  
541 dust, and pollution aerosol on shallow cloud development over the Atlantic Ocean, Proc.  
542 Natl. Acad. Sci., 102, 11207-11212, 2005.

543 Kireeva, E. D., Popovicheva, O. B., Persiantseva, N. M., Khokhlova, T. D., Shonija, N. K.:  
544 Effect of black carbon particles on the efficiency of water droplet freezing, Colloid Journal,  
545 71, 353-359, 2009.

546 Kirstetter, P. E., Andrieu, H., Boudevillain, B., Delrieu, G.: A physically-based identification  
547 of vertical profiles of reflectivity from volume scan radar data, Journal of Applied  
548 Meteorology and Climatology, 52(7), 1645-1663, 2013.

549 Kirstetter, P. E., Andrieu, H., Delrieu, G., Boudevillain, B.: Identification of vertical profiles  
550 of reflectivity for correction of volumetric radar data using rainfall classification, Journal of  
551 Applied Meteorology and Climatology, 49, 2167-2180, 2010.

552 Kock, D., Del Genio, A., D.: Black carbon semi-direct effects on cloud cover: review and  
553 synthesis, Atmospheric Chemistry and physics, 7685-7696, 2010.

554 Koren, I., Martins, J. V., Remer, L. A., Afargan, H.: Smoke invigoration versus inhibition of  
555 clouds over the Amazon: Science, v. 321, 2008.

556 Koren, I., Kaufman, Y. J., Remer, L. A., Martins, J. V.: Measurement of the effect of  
557 Amazon smoke on inhibition of cloud formation, Science, 303, 1342-1345, 2004.

558 Koren, I., Altaratz, O., Remer, L. A., Feingold, G., Martin, V.: Aerosol-induced  
559 intensification of rain from the tropics to the mid-latitudes, Nature Geoscience, 5, 118-122,  
560 2012.

561 Lin, J. C., Matsui, T., Pielke, R. A., and Kummerow, C.: Effects of biomass-burning-derived  
562 aerosol on precipitation and cloud in the Amazon basin: a satellite-based empirical study,  
563 *J. Geophys. Res.*, 111, 1-14, D19204, doi: 10.1029/2005JD006884, 2006.

564 Liu, J., Li, Z.: Estimation of cloud condensation nuclei concentration from aerosol optical  
565 quantities: influential factors and uncertainties *Atmos. Chem. Phys.*, 14, 471–483, 2014.  
566 doi:10.5194/acp-14-471-2014

567 Machado, L. A. T., Laurent, H., Dessay, N., Miranda, I.: Seasonal and diurnal variability of  
568 convection over the Amazonia: A comparison of different vegetation types and large scale  
569 forcing, *Theoretical and Applied Climatology*, 78, 61-77, 2004.

570 Mahowald, N.: Aerosol indirect effect on biogeochemical cycles and climate, *Science*, 224,  
571 794-796, 2011.

572 Marshal, J. S., Palmer, W.: The distribution of raindrops with size, *Journal of Atmospheric*  
573 *Sciences*, 5, 165-166, 1948.

574 Martin, S. T., Andreae, M. O., Artaxo, P., Baumgardner, D., Chen, Q., Goldstein, A. H.,  
575 Guenther, A., Heald, C. L., Mayol-Bracero, O. L., McMurry, P. H., Pauliquevis, T., Poschl,  
576 U., Prather, K. A., Roberts, G. C., Saleska, S. R., Silva Dias, M. A., Spracklen, D. V.,  
577 Swietlicki, E., and Trebs, I.: Sources and properties of Amazonian aerosol particles, *Rev.*  
578 *Geophys.*, 48, 1-42, 2008RG000280, doi:10.1029/2008RG000280, 2010.

579 McFarquhar, G. M., and Heymsfield, A. J.: Parameterizations of INDOEX microphysical  
580 measurements and calculations of cloud susceptibility: Applications for climate studies, *J.*  
581 *Geophys. Res.*, 106, 28,675–28,698, 2001

582 Myhre, G., Stordal, F., Johnsrud, M., Kaufman, Y. J., Rosenfeld, D., Storelvmo, T.,  
583 Kristjannsson, J. E., Berntsen, T. K., Myhre, A., Isaksen, I. S.: Aerosol-cloud interaction  
584 inferred from MODIS satellite data and global aerosol models, *Atmospheric Chemistry and*  
585 *Physics*, 7, 3081-3101, 2007.

586 Petersen, W.,H. Christian, andS. Rutledge(2005),TRMM observations of the global  
587 relationship between ice water content and lightning,*Geophys. Res. Lett.*,**32**, L14819,  
588 doi:10.1029/2005GL023236.

589 Petters, M. D., Parsons, M. T., Prenni, A. J., DeMott, P. J., Kreidenweis, S. M., Carrico, C.  
590 M., Sullivan, A. P., McMeeking, G. R., Levin, E., Wold, C. E., Collett Jr, J. L., and  
591 Moosmuller, H.: Ice nuclei emissions from biomass burning, *J. Geophys. Res.*, 114, 1-10,  
592 D07209, doi:10.1029/2008JD011532, 2009.

593 Qian, Y., Gong, D., Fan, J., Leung, L. R., Bennartz, R., Chen, D., and Wang, W.: Heavy  
594 pollutions suppresses light rain in China: observations and modelling, *J. Geophys. Res.*,  
595 114, 1-16, D00K02, doi: 10.1029/2008JD011575, 2009.

596 Ramanathan, V., Crutzen, P. J., Kiehl, T., Rosenfeld, D.: Aerosols, climate, and the  
597 hydrological cycle, *Science*, 294, 2119-2124, 2001.

598 Randles, C. A., Ramaswamy, V.: Direct and semi-direct impacts of absorbing biomass  
599 burning aerosol on the climate of southern Africa: a Geophysical Fluid Dynamics  
600 laboratory GCM sensitivity study, *Atmospheric Chemistry and Physics*, 9819–9831, 2010.

601 Roberts, G. C., Andreae, M. O., Zhou, J., Artaxo, P: Cloud condensation nuclei in the  
602 Amazon Basin: “Marine” conditions over a continent?, *Geophys. Res. Lett.*, 28, 2807 –  
603 2810, 2001.

604 Rosenfeld, D.: TRMM observed first direct evidence of smoke from forest fires inhibiting  
605 rainfall, *Geophysical Research Letters*, 26, 3150-3108, 1999.

606 Rosenfeld, D., Lohmann, U., Raga, G. B., O’Dowd, C. D., Kulmala, M., Fuzzi, S., Reissel,  
607 A., Andreae, M. O.: Flood or drought: How do aerosols affect precipitation? *Science*, 321,  
608 1309-1313, 2008.

609 Ryu, S. Y., Kwon, B. G., Kim, Y. J., Kim, H. H., Chun, K. J.: Characteristics of biomass  
610 burning aerosol and its impact on regional air quality in the summer of 2003 at Gwangju,  
611 Korea, *Atmospheric Research*, 84, 362–373, 2007.

612 Simpson, J., Wiggert, V.: Models of precipitating cumulus towers, *Monthly Weather*  
613 *Review*, 97, 471–489, 1969.

614 Slowik, J. G., Cross, E. S., Han, J., Davidovits, P., Onasch, T. B., Jayne, J. T., Williams, L.  
615 R., Canagaratna, R., Worsnop, D. R., Chakrabarty, R. K., Moosmüller, H., Arnott, W. P.,  
616 Schwarz, J. P., Gao, R., Fahey, D. W., Kok, G. L., and Petzold, A.: An inter-comparison of  
617 instruments measuring black carbon content of soot particles , *Aerosol Sci. Tech.*, 41, 295–  
618 314, 2007.

619 Storelvmo, T.: Uncertainties in aerosol direct and indirect effects attributed to uncertainties  
620 in convective transport parameterizations, *Atmospheric Research*, 118 357-369, 2012.

621 Storer, R. L., Heever, S. C. V. D.: Microphysical processes evident in forcing of tropical  
622 deep convective clouds, *Journal of the Atmospheric Sciences*, 70, 430-446, 2013.

623 Tao, W-K., Chen, J-P., Li, Z., Wang, C., Zhang, C.: Impact of aerosol on convective clouds  
624 and precipitation, *Reviews of Geophysics*, 50, 1-62, 2012.

625 Tegen, I., Hollrig, P., Chin, M., Fung, I., Jacob, D., Penner, J.: Contribution of different  
626 aerosol species to the global aerosol extinction optical thickness: Estimates from model  
627 results, *J. Geophys. Res.*, 102, 895-915, 1997.

628 Tiwari, S., Srivastava, A. K., Bisht, D. S., Parmita, P., Srivastava, M. K., Attri, S. D.: Diurnal  
629 and seasonal variations of black carbon and PM<sub>2.5</sub> over New Delhi, India: Influence of  
630 meteorology *Atmospheric Research* 125–126 50–62, 2013.

631 Vila, D. A., Machado, L. A. T., Laurent, H., Velasco, I.: Forecast and Tracking the Evolution  
632 of Cloud Clusters (ForTraCC) using satellite infrared imagery, methodology and validation,  
633 *Weather and Forecasting*, 23, 233-245, 2008.

634 Wake, B.: Aerosol-driven warming, *Nature Climate Change*, 2, 570-571, 2012.

635 Wallace, J. M. and Hobbs, P. V.: *Atmospheric Science: an Introductory Survey*, Academic  
636 Press, San Diego, California, USA, 2006.

637 Wang, C.: Impact of anthropogenic absorbing aerosols on clouds and precipitation: A  
638 review of recent progresses, *Atmospheric Research*, 122, 237–249, 2013.

639 Yum, S. S., and J. G. Hudson (2002), Maritime/continental microphysical contrasts in  
640 stratus, *Tellus, Ser. A and Ser. B*, 54B, 61–73.

641

642

643

644

645

646

647

648

649

650

651

652

653

654

655

656

657

658 **Figures and Tables**

659

660 Table 1. Observed features and proposed mechanisms for stable and unstable atmospheres during  
 661 the dry and wet seasons.

| <b>Atmosphere State<br/>Wet season</b> | <b>Observed Features</b>   | <b>Possible Mechanisms Explaining<br/>this behaviour:</b>   |
|--|--|---|
| Less Unstable<br>(CAPE<1400 J/kg )     | <ul style="list-style-type: none"> <li>- Rain and Ice Fraction decreases as BC increases ;</li> <li>- Low BC concentration;</li> <li>- No influence on rain cell size;</li> </ul>  | <ul style="list-style-type: none"> <li>- The wet scavenging process, greater formation of cloud droplets with reduced size suppressing precipitation;</li> <li>- Atmosphere stabilization;</li> </ul>   |
| More Unstable<br>(CAPE>2600 J/kg)      | <ul style="list-style-type: none"> <li>- Rain and Ice Fraction decreases as BC increases;</li> <li>- Low BC concentration;</li> <li>- No influence on rain cell size;</li> </ul>   | <ul style="list-style-type: none"> <li>- The wet scavenging process, greater formation of cloud droplets with reduced size suppressing precipitation;</li> </ul>  |
| <b>Atmosphere State<br/>Dry season</b> | <b>Observed Features</b>   | <b>Possible Mechanisms Explaining<br/>this behaviour:</b>   |
| Less Unstable<br>(CAPE<1400 J/kg )     | <ul style="list-style-type: none"> <li>- Rain and Ice Fraction decreases as BC increases;</li> <li>- High polluted atmosphere (&gt;1000 ng/m<sup>3</sup>);</li> <li>- No influence on rain cell size;</li> </ul>   | <ul style="list-style-type: none"> <li>- The wet scavenging process, greater formation of cloud droplets with reduced size suppressing precipitation;</li> <li>- Atmosphere stabilization;</li> <li>- Less buoyancy;</li> <li>- Weaker updrafts;</li> <li>- Weaker homogenous ice formation;</li> </ul> |
| More Unstable<br>(CAPE>2600 J/kg)      | <ul style="list-style-type: none"> <li>- Rain and Ice Fraction increases as BC increases;</li> <li>- High polluted atmosphere (&gt;1000 ng/m<sup>3</sup>);</li> <li>- Increase of rain cell size as BC increases, only for large rain cell areas (&gt;100 km<sup>2</sup>)</li> </ul> | <ul style="list-style-type: none"> <li>- High buoyancy;</li> <li>- Stronger updrafts;</li> <li>- High homogenous ice formation;</li> <li>- More latent heating;</li> <li>- Convection invigorated;</li> <li>- Smaller entrainment for large rain cells</li> </ul>                                       |

662

663

664

665

666

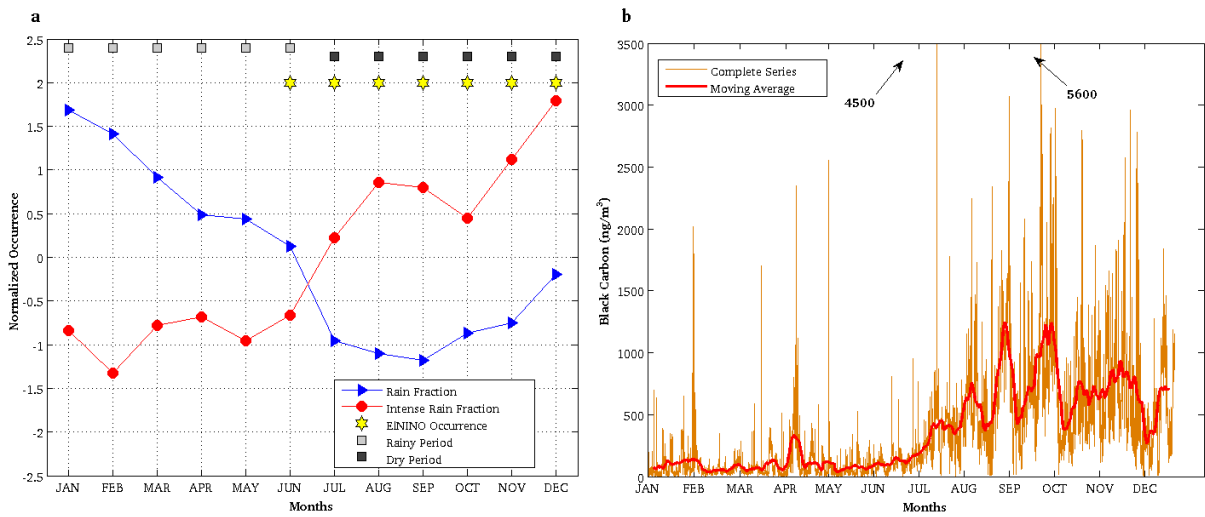


Figure 1. (a) Annual cycle of rain fraction (RF) and intense rain fraction (IRF) values normalized by their annual means and standard deviations for the S-band radar located in Manaus in 2009. The symbols at the top of the panel represent the rainy period (light gray squares), the dry period (dark gray squares), and El Niño occurrence (yellow stars). (b) Annual cycle of black carbon (BC) for Manaus in 2009. The orange line represents the complete series in 30-minute intervals for each measurement, and the thick red line represents a weekly moving average.

667

668

669

670

671

672

673

674

675

676

677

678

679

680

681

682

683

684

685

686

687

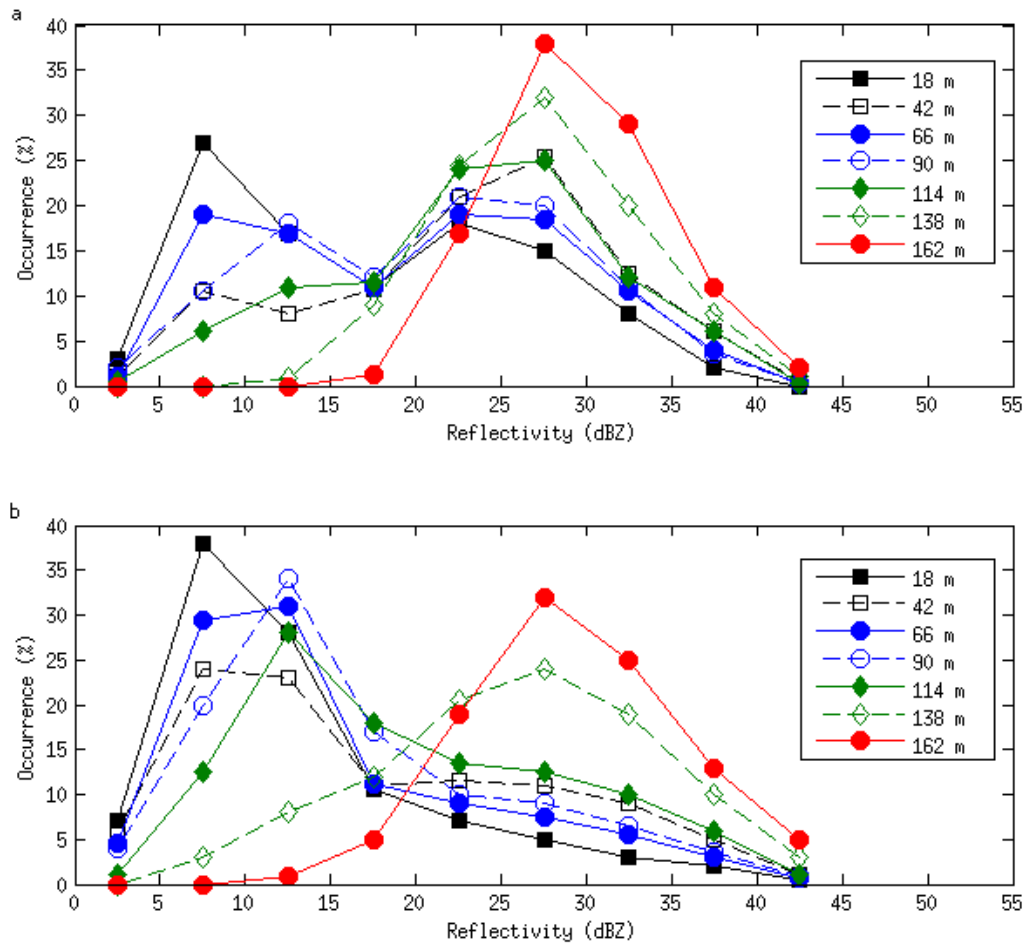


Figure 2. Frequency histograms of radar reflectivity for different topography elevations (intervals of 24 m) for the S-band radar located in Manaus in 2009. (a) Rainy season; (b) Dry season.

688  
 689  
 690  
 691  
 692  
 693  
 694  
 695  
 696  
 697  
 698  
 699

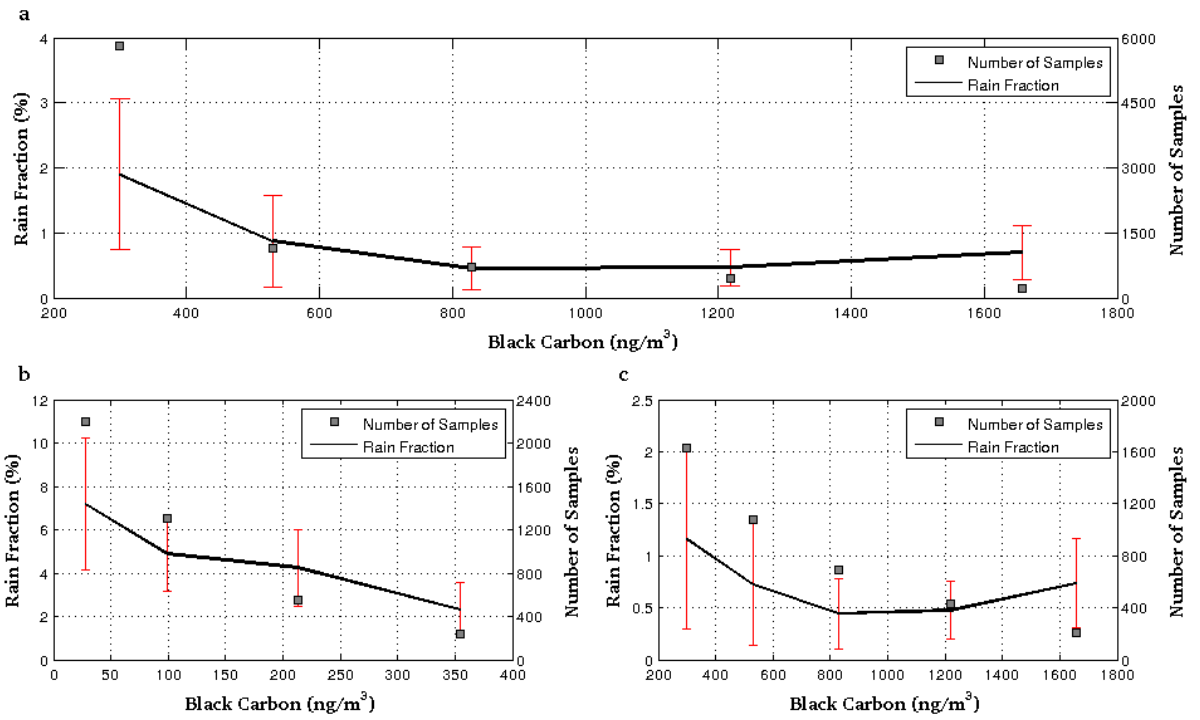


Figure 3. Mean, standard deviation and number of samples of rain fraction (RF) for different black carbon (BC) concentrations. (a) Entire year; (b) Rainy Season; (c) Dry season. For these curves, no atmospheric stability consideration was performed.

701

702

703

704

705

706

707

708

709

710

711

712

713

714

715

716



717

718

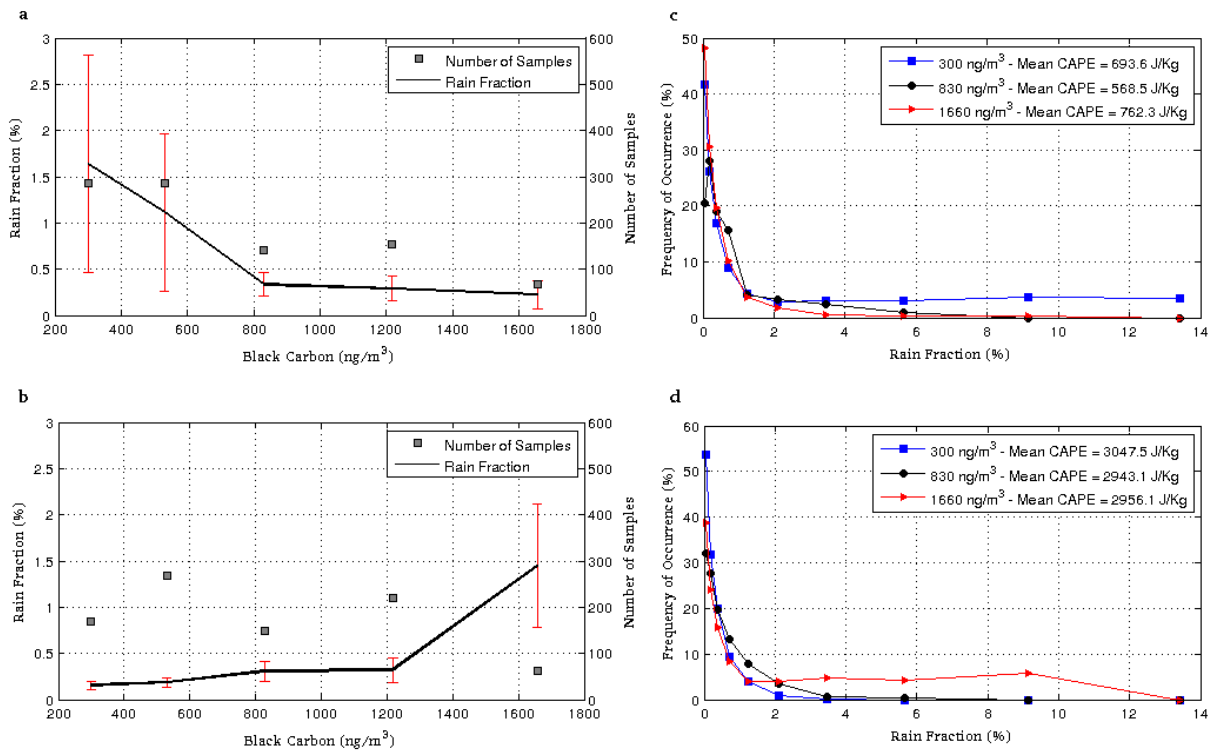


Figure 4. Mean, standard deviation and number of samples of rain fraction (RF) for different black carbon (BC) concentrations for less unstable (a) and more unstable (b) atmospheres in the dry period. RF frequency histograms for the first, third and fifth BC concentrations in (a) and (b), are shown for less unstable (c) and more unstable (d) atmospheres. The first and third curves in (c) and (d) are significantly different as determined by a t-test at the 95% confidence level.

719

720

721

722

723

724

725

726

727

728

729

730

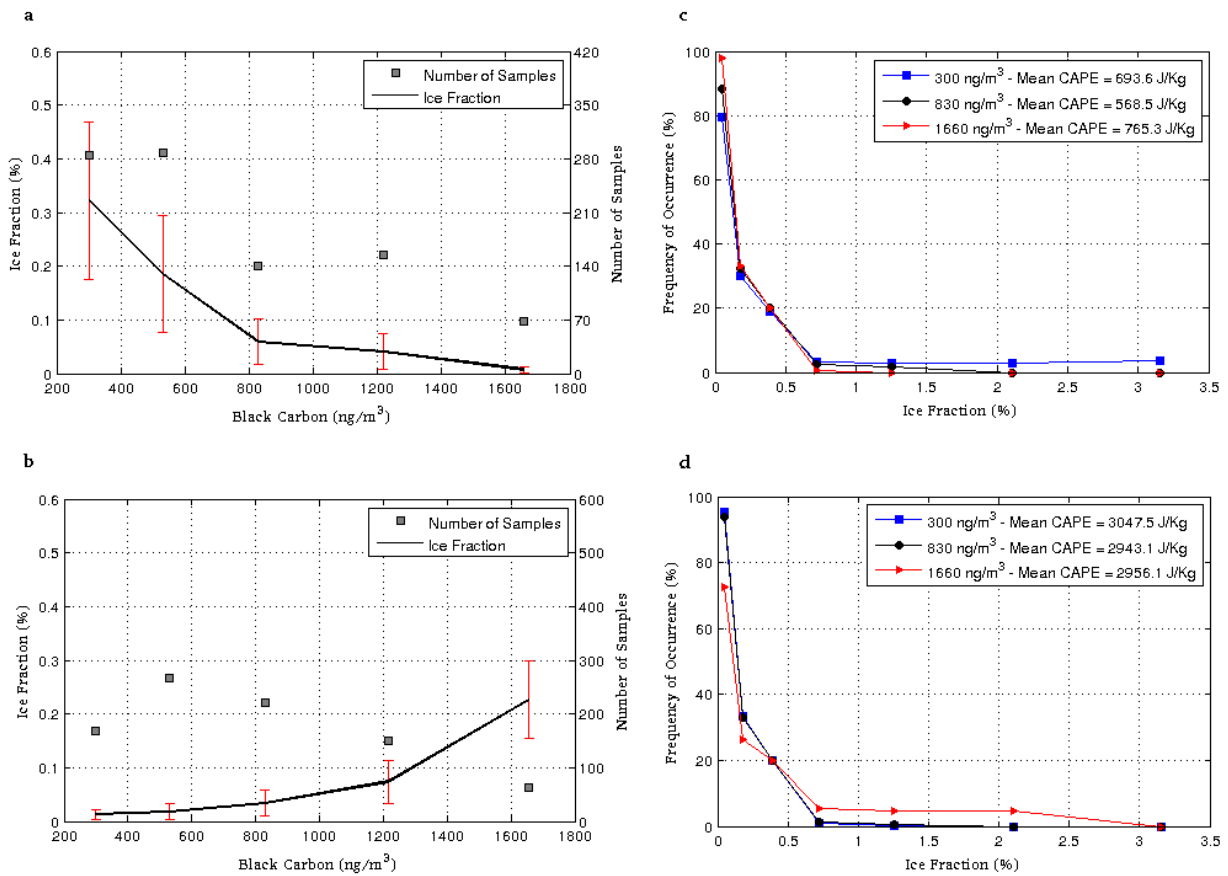


Figure 5. Mean, standard deviation and number of samples of ice fraction (IF) for different black carbon (BC) concentrations for stable (a) and unstable (b) atmospheres in the dry period. IF frequency histograms for the first, third and fifth BC concentrations in (a) and (b) are shown for less unstable (c) and more unstable (d) atmospheres. The first and third curves in (c) and (d) are significantly different at as determined by a t-test at the 95% confidence level.

731  
 732  
 733  
 734  
 735  
 736  
 737  
 738  
 739  
 740  
 741

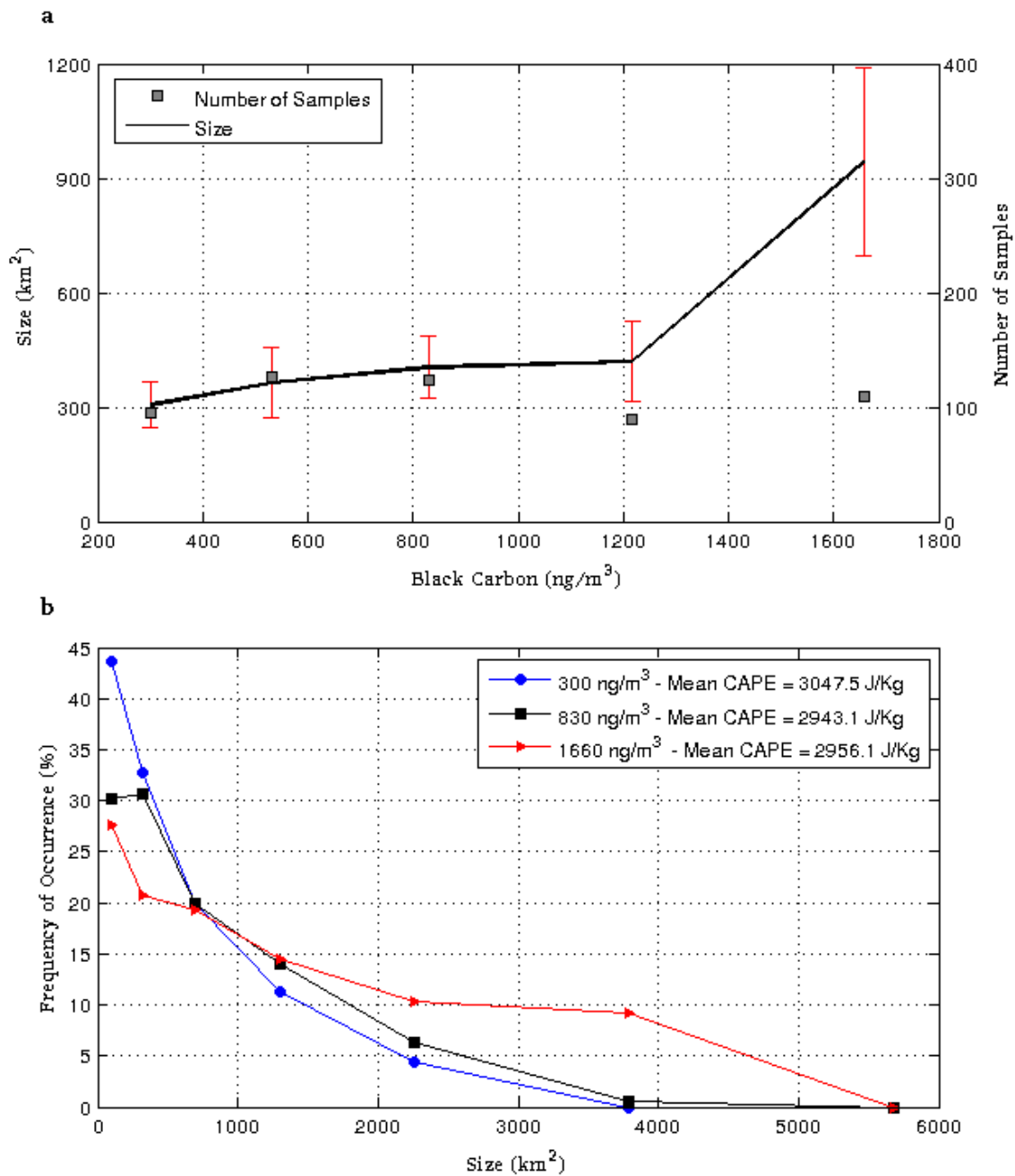


Figure 6. (a) Mean, standard deviation and number of samples of rain cell size ( $>100 \text{ km}^2$ ) for different black carbon (BC) concentrations in a more unstable atmosphere during the dry period; (b) Size frequency histograms for the first, third and fifth BC concentrations in (a). The first and third curves in (b) are significantly different as determined by a t-test at the 95% confidence level.